Supplementary Information

Online Methods

Supplementary Figs. S1-7

Supplementary figure legends

Supplementary Tables S1 and S2

Supplementary Methods

Generation of *auf1*$^{-/-}$ mice

All *auf1*$^{-/-}$ KO mice and WT mice are of the 129/B6-background at F3 and F4 generation breeds from *auf1*$^{+/-}$ heterozygous mice. Ages varied from 3-12 months and are specified for each procedure (Lu and Schneider, 2004; Pont et al., 2012; Sadri and Schneider, 2009).

Actinomycin D treatment

C2C12 cells were treated with 0.2 µg/ml actinomycin D (Sigma) for up to 2 h. RNA was extracted using Trizol as per manufacturer instructions. cDNA was generated using Promega GoScript reverse transcription system as per manufacturer instructions. qRT-PCR was completed using an Applied Biosystems 7500 Fast RT-PCR machine as per manufacture instructions. Experiments were analyzed in triplicate, then means and standard deviations calculated.

Quantitative real-time PCR (qRT-PCR) and analysis

RNA was extracted using Trizol as per manufacturer instructions. cDNA was generated using Promega GoScript reverse transcription system as per manufacturer instructions. qRT-PCR was completed using an Applied Biosystems 7500 Fast RT-PCR machine as per manufacture instructions. Data were analyzed by comparative CT values with *GapDH* as an internal control.

Immunoblot studies

In brief, cells were lysed in RIPA buffer or media was collected. Lysate was resolved by 12% PAGE and transferred overnight to a PVDF transfer membrane (Millipore). Membrane was blocked in 5% milk in TBS. Primary antibodies were incubated at 4^{o}C overnight. Secondary ECL antibodies (GE Healthcare) were incubated for 1 h at room temperature. Protein was imaged using Thermoscientific SuperSignal and Genemate autoradiography film. The following antibody dilutions were used: rabbit antibody to AUF1 (Millipore, 07-260, 1:500), rabbit antibody to GapDH (Cell Signaling, 2118, 1:1000), rabbit antibody to cyclin D1 (Cell Signaling, 2922, 1:1000), mouse antibody to PAX7 (*in vivo:* DSHB 1:500; *in vitro:* Santa Cruz Biotechnology, SC-81648, 1:500)

RNA-seq bioinformatics analysis

Sequenced fragments were quality controlled by examination using FAST-QC, and to assure removal of mitochondrial RNA, tRNAs and ribosomal RNAs, then aligned to the human reference genome using *Bowtie* (Langmead et al., 2009) and other alignment tools for short read alignment, *TopHat* for alignment to reference genomes for splice site locations (Trapnell et al., 2009; Trapnell and Salzberg, 2009), low counts filtered using *HtSeq Rawcounts*, and to quantify counts per gene, data normalized using the *Voom* function on the R-limma package, which examines mean variance for each gene to achieve normal distribution by lowest variance, then transcripts assembled and compared or merged with other short sequence reads using *Cufflinks* (Trapnell et al., 2010). *Limma differential expression* was used to compare total mRNA data sets as $\log_2$ ratios and significance of mRNAs will be assessed using *P*-values, fold changes and the FDRs estimated based on t-tests. Studies were performed from 3 independent data sets. Other types of statistical analyses included supervised and unsupervised clustering and metabolic and biochemical pathway groupings using the *Intuition software* package.

Microarrays and data analysis. Purified mRNAs (50ng) from total or polysomal associated fractions were processed using the GeneChip WT PLUS Reagent Kit and hybridized to Human Transcriptome Array 2.0 chips from Affymetrix according to the manufacturer's instructions. Gene-level probeset summary of microarray data were obtained using the GCCN and SST transformation algorithm, RMA background correction, and quantile normalization provided in Expression Console Software, version 1.4.1 (Affymetrix). Control probesets and probesets lacking mRNA accession tags were removed from futher analysis. To quantify translational efficiency, the difference in $\log_2$ intensity between matched polysomal RNA and total RNA was determined. To examine differences in transcription and translation, total RNA and polysome RNA were quantile normalized separately. Statistical analysis was performed using the limma R package (Ritchie et al., 2015).

References

Langmead, B., Trapnell, C., Pop, M., and Salzberg, S.L. (2009). Ultrafast and memory-efficient alignment of short DNA sequences to the human genome. Genome biology *10*, R25.

Lu, J.Y., and Schneider, R.J. (2004). Tissue distribution of AU-rich mRNA-binding proteins involved in regulation of mRNA decay. The Journal of biological chemistry *279*, 12974-12979.

Pont, A.R., Sadri, N., Hsiao, S.J., Smith, S., and Schneider, R.J. (2012). mRNA decay factor AUF1 maintains normal aging, telomere maintenance, and suppression of senescence by activation of telomerase transcription. Molecular cell *47*, 5-15.

Ritchie, M.E., Phipson, B., Wu, D., Hu, Y., Law, C.W., Shi, W., and Smyth, G.K. (2015). limma powers differential expression analyses for RNA-sequencing and microarray studies. Nucleic Acids Res *43*, e47.

Sadri, N., and Schneider, R.J. (2009). Auf1/Hnrnpd-deficient mice develop pruritic inflammatory skin disease. The Journal of investigative dermatology *129*, 657-670.

Trapnell, C., Pachter, L., and Salzberg, S.L. (2009). TopHat: discovering splice junctions with RNA-Seq. Bioinformatics *25*, 1105-1111.

Trapnell, C., and Salzberg, S.L. (2009). How to map billions of short reads onto genomes. Nature biotechnology *27*, 455-457.

Trapnell, C., Williams, B.A., Pertea, G., Mortazavi, A., Kwan, G., van Baren, M.J., Salzberg, S.L., Wold, B.J., and Pachter, L. (2010). Transcript assembly and quantification by RNA-Seq reveals unannotated transcripts and isoform switching during cell differentiation. Nat Biotechnol *28*, 511-515.

Chenette et al., Supplementary Figure 1 - Related to Figure 1

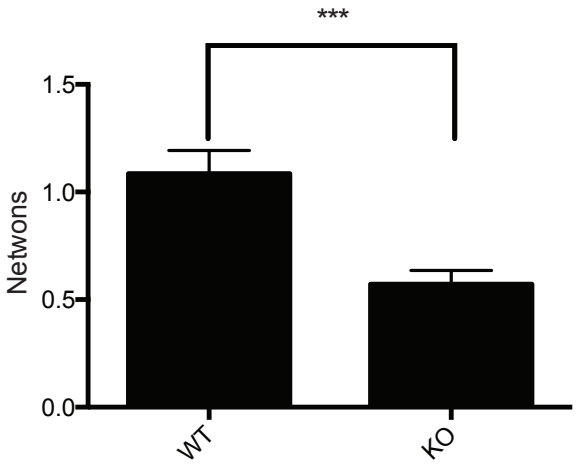

Chenette et al., Supplementary Figure 2 - Related to Figure 2

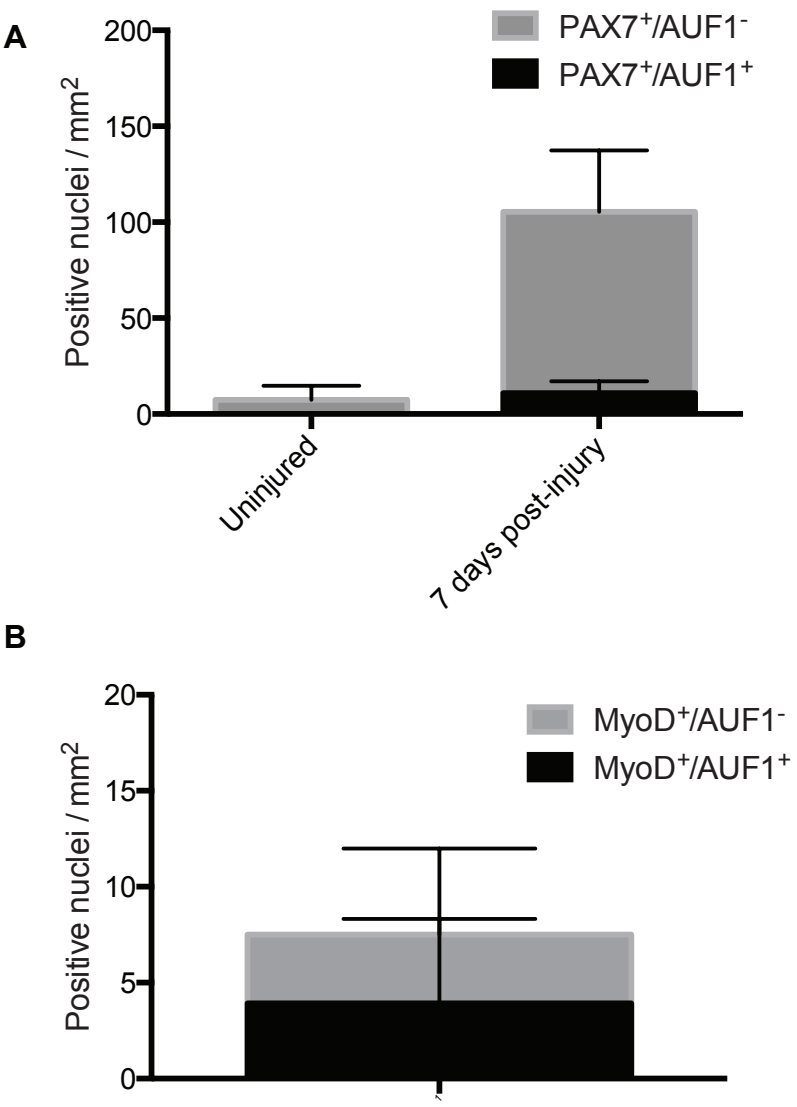

Chenette et al., Supplementary Figure 3 - Related to Figure 2

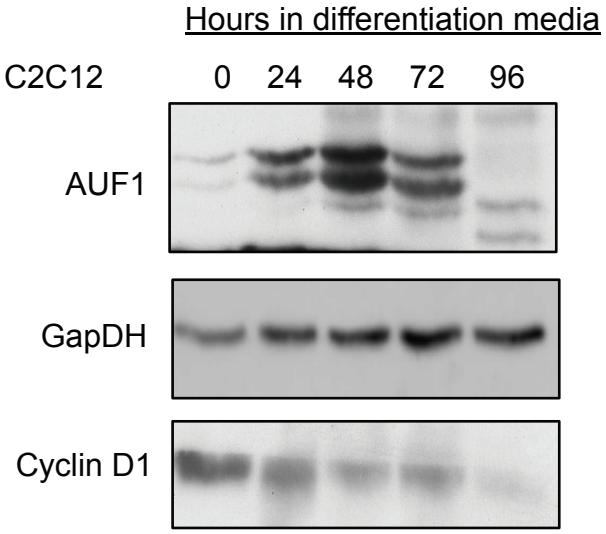

Chenette et al., Supplementary Figure 4 - Related to Figure 3

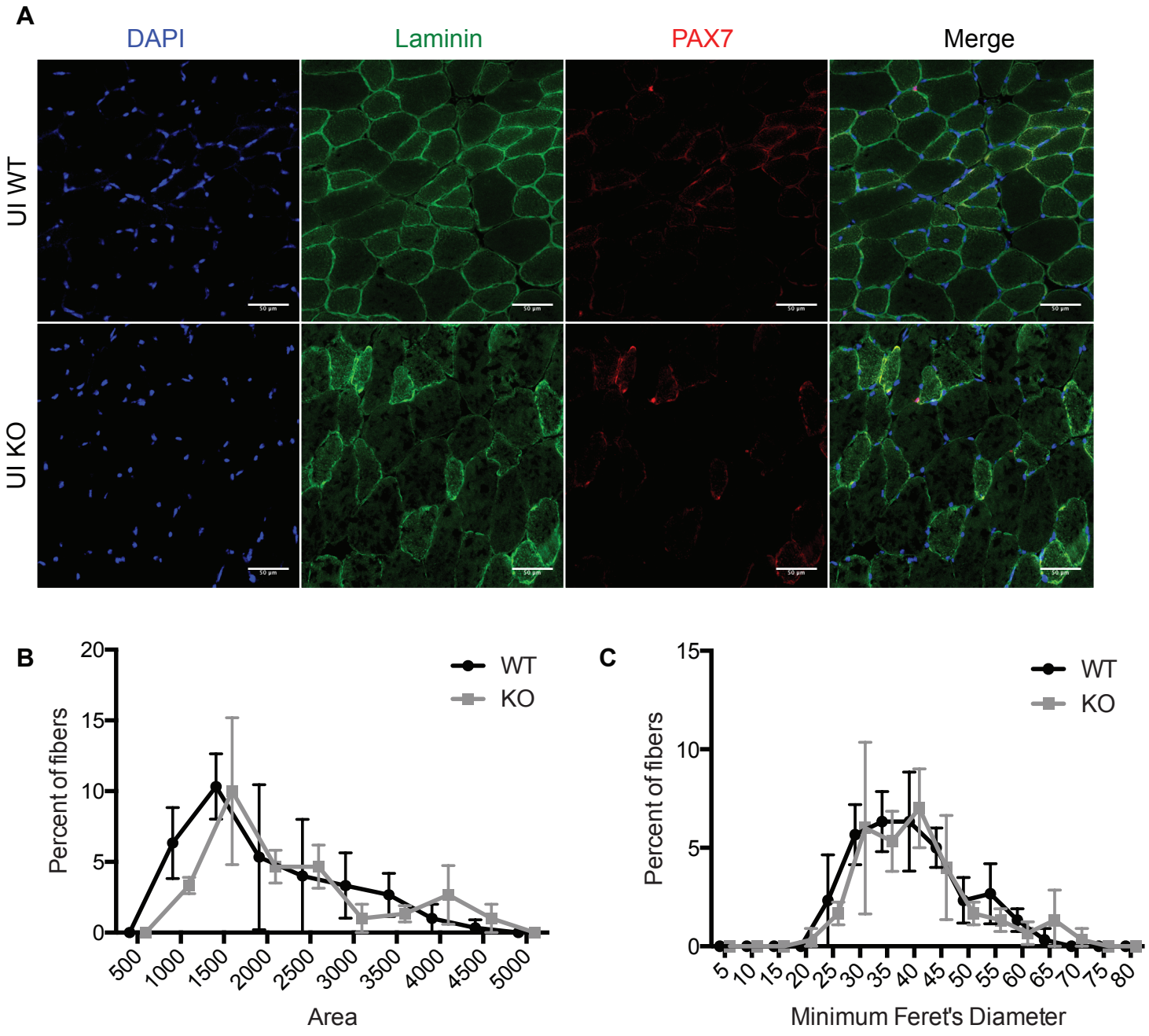

Chenette et al., Supplementary Figure 5 - Related to Figure 4

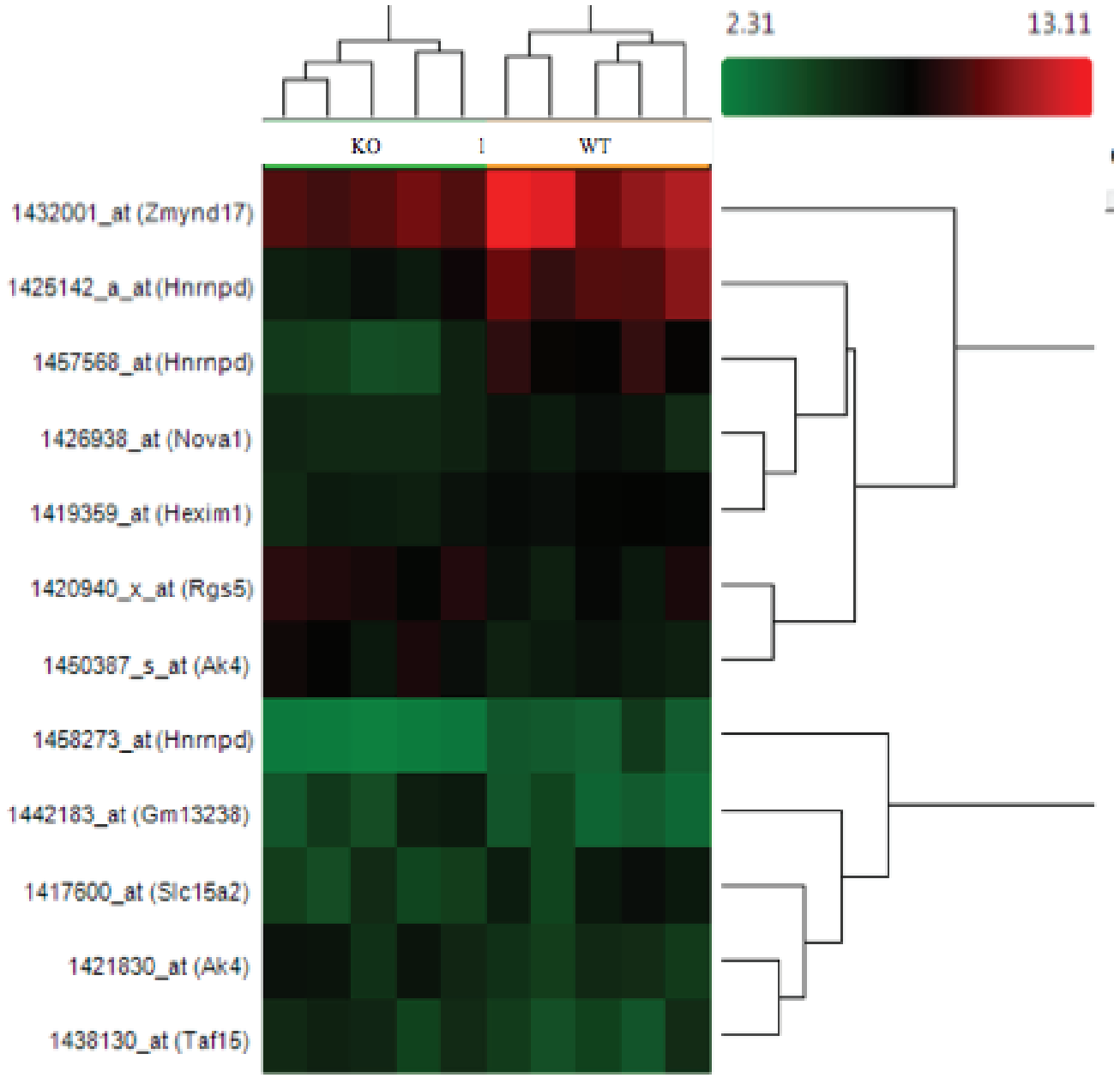

Chenette et al., Supplementary Figure 6 - Related to Figure 4

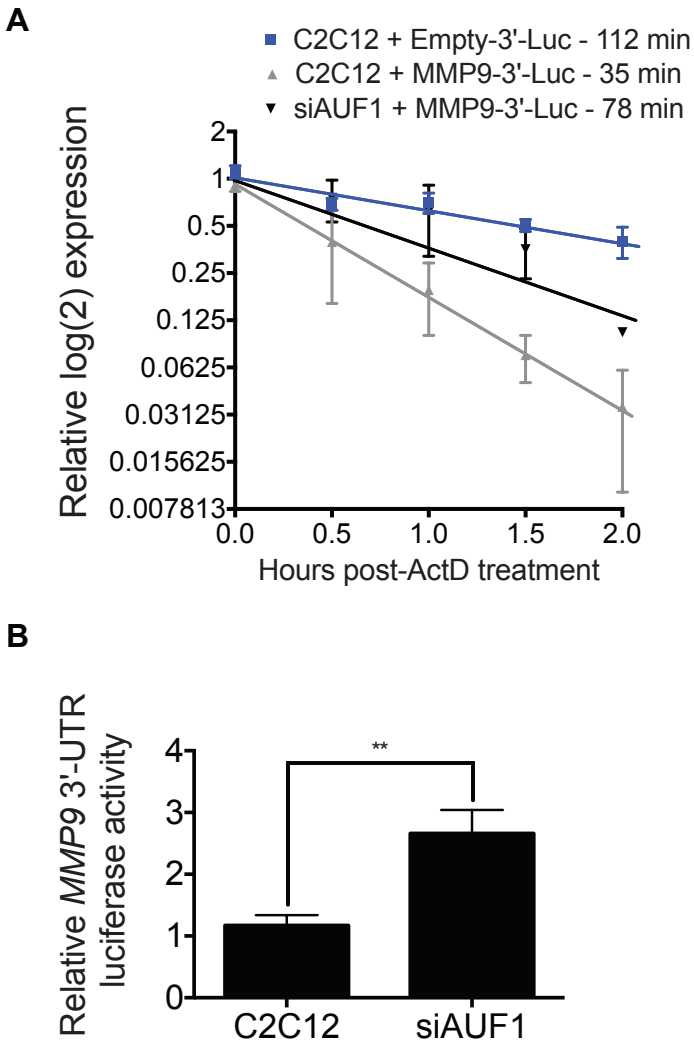

Chenette et al., Supplementary Figure 7 - Related to Figure 4

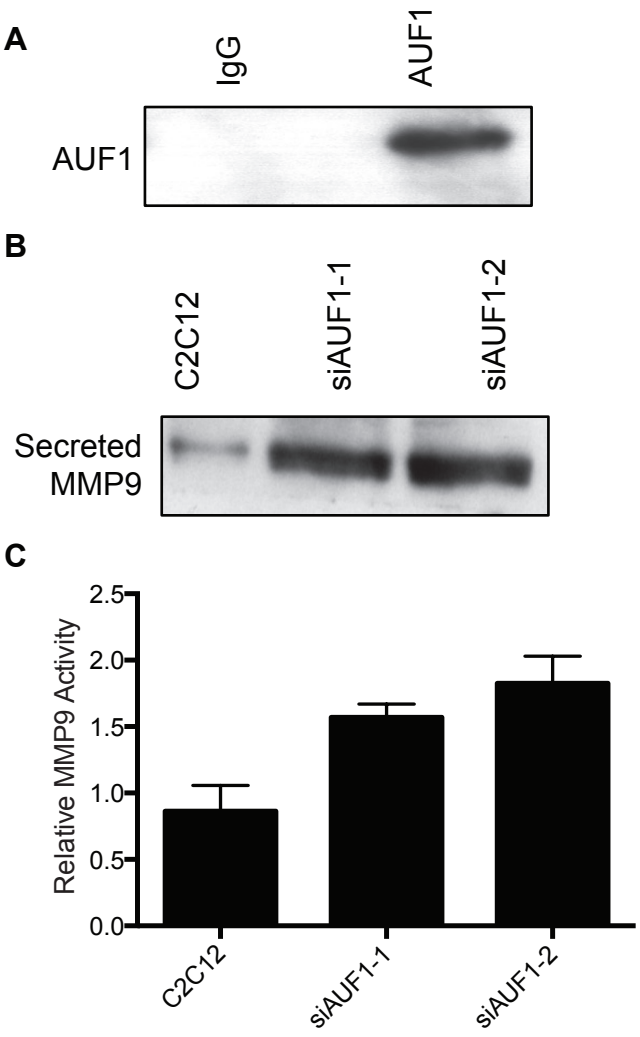

Supplementary Figure 1, related to Figure 1 Aging KO mice are significantly weaker than WT mice – Related to Figure 1. Strength grip analysis of 4-8 month old mice. Five mice per genotype were tested in triplicate. $P<0.0005$, unpaired t-test.

Supplementary Figure 2, related to Figure 2 AUF1 is expressed in MyoD+ satellite cells – Related to Figure 2. **(A)** Quantification of AUF1 co-localization to PAX7 in uninjured and 7 days post-injury TA muscle showing AUF1 is expressed in a subset of PAX7+ satellite cells. (**B**) Quantification of AUF1 co-localization with MyoD in cultured myofibers showing AUF1 is expressed in over 50% of MyoD+ satellite cells.

Supplementary Figure 3, related to Figure 2 AUF1 is expressed in C2C12 cells. Protein levels of AUF1 were probed in differentiating C2C12 cells – Related to Figure 2. Cells were differentiated through serum starvation by growing to confluence and culturing in 2% horse serum. Time points were analyzed in triplicate. 50 μg of protein were loaded per time point.

Supplementary Figure 4, related to Figure 3 4 month old KO skeletal muscle is not morphologically distinct from WT skeletal muscle prior to injury – Related to Figure 3. (**A**) Immunofluorescence staining for the expression of laminin (AF488, green), PAX7 (AF555, red), and nuclei (DAPI ,blue) in 4 month old uninjured TA muscle. TA muscles were frozen in OCT, 5 images from 3 sections were analyzed per mouse and 3 mice were studied per genotype (scale bar 50 μm). (**B**) Quantification of fiber size by area in uninjured TA muscle. Fiber area was calculated by ImageJ64. Five images from 3 sections were analyzed per mouse and 3 mice were studied per genotype (ns, 2 way ANOVA). (**C**) Quantification of fiber size by Minimum Feret's Diameter in uninjured TA muscle. Fiber Minimum Feret's Diameter was calculated by ImageJ64. Five images from 3 sections were analyzed per mouse and 3 mice were studied per genotype (ns, 2 way ANOVA).

Supplementary Figure 5, related to Figure 4 MMP9 expression is not altered in bulk skeletal muscle – Related to Figure 4. Heat map of Affymetrix data from whole hindlimb

skeletal muscle. Whole hindlimb skeletal muscle from WT and KO 6 month old mice was surgically removed and RNA was extracted from the fibers according to manufacturer's instructions (TRIzol). Muscle was isolated from 5 mice per genotype. RNA was cleaned using RNeasy Mini Elute Kit (Qiagen) and analyzed on Affymetrix chips. Twelve genes were differentially expressed, significantly fewer than in satellite cells. Upregulated genes are shown in red and downregulated genes are shown in green.

Supplementary Figure 6, related to Figure 4 AUF1 promotes the destabilization of *MMP9* through ARE-rich regions in the 3'UTR – Related to Figure 4. (**A**) The longest ARE-repeat (~200 kB) was cloned into the 3-UTR of a luciferase reporter pzeo-luc vector. This plasmid (MMP9-3'-LUC) or an empty plasmid (Empty-3'-Luc) was transient transfected in untreated (C2C12) or siAUF1 treated (siAUF1) C2C12 cells for 48 hours. Cells were then treated with ActD for up to 4 hours. RNA was harvested using Trizol and analyzed with qRT-PCR analysis. (**P<0.005, *P<0.05, unpaired t-test). (**B**) In non-ActD treated cells, luciferase activity was measured using a Dual Luciferase Report Assay (Promega). (**P<0.005, unpaired t-test).

Supplementary Figure 7, related to Figure 4 High levels of MMP9 are secreted in the partial absence of AUF1 – Related to Figure 4. (A) Protein levels of AUF1 were probed following AUF1 immunoprecipitation with either anti-AUF1 or rabbit IgG (Santa Cruz) antibodies in C2C12 cells by immunoblot. Immunoprecipitation was analyzed in triplicate. 50 μg of protein were loaded. (**B**) Protein levels of secreted MMP9 were probed from the media of cultured C2C12 cells treated with either vehicle or siAUF1. Two siAUF1 sequences were used. Experiments were performed in triplicate. 50 μg of protein were loaded. (**C**) Quantification of MMP9 activity using EnzChek ELISA activity assay. Media was tested from C2C12 cells treated with vehicle or siAUF1. Two siAUF1 sequences were used. Experiments were performed in triplicate.

Table S1: mRNAs altered in expression in AUF1$^{-/-}$ satellite cells

Gene	log2	ARE
Acan	Undetected in WT	**
Clec3a	Undetected in WT	
Glrb	Undetected in WT	**
Gm10451	Undetected in WT	
Nudt10	Undetected in WT	
Rbp2	Undetected in WT	
Serpinb7	Undetected in WT	**
Gm10664	Undetected in WT	
Gpr143	Undetected in WT	
Ifng	Undetected in WT	**
Il17a	Undetected in WT	**
Lrrc6	Undetected in WT	**
Nxf7	Undetected in WT	
Olfr561	Undetected in WT	*
Rnaset2b	Undetected in WT	
Serpina11	Undetected in WT	
Slc9a4	Undetected in WT	**
Upk3a	Undetected in WT	
Il10	4.39043	**
1100001G20Rik	3.95336	
S100a8	3.92684	
S100a9	3.84433	
Mmp8	3.64128	
Camp	3.62679	
Ly6c2	3.50382	*
Chi3l3	3.49607	
Retnlg	3.49241	
Slpi	3.48521	*
Igj	3.45704	**
Trem3	3.45536	
Ngp	3.39607	
Fpr1	3.33711	
Hp	3.32877	
Prg2	3.29363	
Ltf	3.25381	**
Mpo	3.24544	
Ms4a4c	3.1774	**
Ifitm6	3.16461	*
Lcn2	3.1227	
Fcnb	3.05636	
Clec4d	3.05123	**
Sell	3.03807	
Nkg7	3.03528	
1810033B17Rik	2.93916	
Cd177	2.93699	
BC018473	2.80585	
Il1rn	2.76114	
Ccl8	2.75957	
Clec4e	2.72767	

Irg1	2.69337	*
Epx	2.67661	*
Ifi27l2a	2.55783	
Cyp1a1	2.53325	
Cd52	2.50045	
Samsn1	2.40563	**
Ccr7	2.39861	
Ccnb2	2.36848	
Il1r2	2.34967	
Cyp4f18	2.31217	
Slfn4	2.26772	**
Parvg	2.24493	
Rdh12	2.22375	*
Fgr	2.22284	**
Oasl1	2.18429	
Trem1	2.1539	
Napsa	2.09279	
Rac2	1.9299	
H19	1.90029	
Pglyrp1	1.87053	
Mmp9	1.80339	**
Coro1a	1.79058	
Ccr2	1.77478	**
Cytip	1.75695	
Ncf1	1.75443	**
Adam8	1.70573	
Il1b	1.67181	**
Chi3l1	1.66464	
Irf7	1.6173	
G0s2	1.60887	
Tyrobp	1.58677	
Plaur	1.32265	**
Ret	-1.61664	
Zer1	-1.6413	
Gbp1	-1.96314	**
Nxpe4	-2.0992	**
Erdr1	-2.12255	
Plvap	-2.27937	*
Nuak1	-2.5782	**
Col11a1	-2.59413	**
Hal	-2.78574	**
Col2a1	-4.97584	**

mRNAs altered in abundance in satellite cells as determined by RNA-Seq analysis. Ninety-one genes were identified, indicated by the gene abbreviated name, and the log2 fold change from RNA-Seq analysis was reported. Transcripts containing probable ARE sequences in the 3'UTR are marked with an asterisk (*). Transcripts containing at least two ARE pentames are marked with two asterisks (**). Transcripts decreased in abundance are indicated by a minus sign.

Table S2: Known AUF1 ARE-mRNA targets altered in expression in AUF1$^{-/-}$ satellite cells

Gene	AREs	Fold change	Linked to skeletal muscle regeneration
CCR2	10	3.4	Y
Col11a1	12	-5	N
IL17a	13	Undetected in WT	N
MMP9	11	3.6	Y

Identification of known AUF1 target mRNAs altered in AUF1$^{-/-}$ satellite cells. Genes significantly altered in the AUF1$^{-/-}$ satellite cells detected by RNA-Seq analysis were subject to in silico characterization for known AUF1 association. Four genes were identified. Shown are the gene abbreviated name, number of predicted AUF1-targeted ARE motifs in the mRNA 3'UTR, the fold change extrapolated from the log2 change calculated from RNA-Seq analysis, and whether the gene has been linked to skeletal muscle regeneration (Y = Yes, N = No). Genes decreased in abundance are indicated by a minus sign.